MOLECULAR AND CELLULAR BIOLOGY, Oct. 2004, p. 9038–9047 Vol. 24, No. 20
0270-7306/04/$08.00+0 DOI: 10.1128/MCB.24.20.9038–9047.2004

Vhlh Gene Deletion Induces Hif-1-Mediated Cell Death in Thymocytes†

Mangatt P. Biju,[1]‡ Aaron K. Neumann,[1,2]‡ Steven J. Bensinger,[1,2] Randall S. Johnson,[3] Laurence A. Turka,[1,2] and Volker H. Haase[1,4]*

Department of Medicine[1] and Immunology Graduate Group[2] and Cell and Molecular Biology Graduate Group, Program in Cell Growth and Cancer,[4] University of Pennsylvania, Philadelphia, Pennsylvania, and Molecular Biology Section, Division of Biology, University of California San Diego, La Jolla, California[3]

Received 17 December 2003/Returned for modification 27 February 2004/Accepted 19 July 2004

The von Hippel-Lindau gene product (pVHL) targets the α subunit of basic helix-loop-helix transcription factor hypoxia-inducible factor (HIF) for proteasomal degradation. Inactivation of pVhl in the mouse germ line results in embryonic lethality, indicating that tight control of Hif-mediated adaptive responses to hypoxia is required for normal development and tissue function. In order to investigate the role of pVhl in T-cell development, we generated mice with thymocyte-specific inactivation of *Vhlh* resulting in constitutive transcriptional activity of Hif-1, as well as mice with thymocyte-specific repression of Hif-1 in a wild-type and *Vhlh*-deficient background. Thymi from *Vhlh*-deficient mice were small due to a severe reduction in the total number of CD4/CD8-double-positive thymocytes which was associated with increased apoptosis in vivo and in vitro. Increased apoptosis was a result of enhanced caspase 8 activity, while Bcl-2 and Bcl-X_L transgene expression had little effect on this phenotype. Inactivation of Hif-1 in *Vhlh*-deficient thymocytes restored thymic cellularity as well as thymocyte viability in vitro. Our data suggest that tight regulation of Hif-1 via pVhl is required for normal thymocyte development and viability and that an increase in Hif-1 transcriptional activity enhances caspase 8-mediated apoptosis in thymocytes.

Thymocytes are exposed to regional hypoxia while they develop into mature T cells (20); how they adapt to low levels of oxygen is not well understood. Hypoxia-inducible factors (HIFs) are key mediators of the cell's response to hypoxia. HIF-α subunits are targeted for ubiquitination and subsequent proteasomal degradation by the ubiquitously expressed von Hippel-Lindau gene product (pVHL), which is the substrate recognition component of an E3 ubiquitin ligase (24, 25, 27, 38, 50). HIF-1 and HIF-2 facilitate both oxygen delivery and adaptation to oxygen deprivation by regulating genes that are involved in glucose uptake and metabolism, angiogenesis, erythropoiesis, cell proliferation, and apoptosis (55, 65). Both factors belong to the PAS (Per-ARNT-Sim) family of basic helix-loop-helix transcription factors and bind DNA as heterodimers composed of an oxygen-sensitive α subunit and a constitutively expressed β subunit, also known as the aryl hydrocarbon receptor nuclear translocator (ARNT) or HIF-β. HIF-1α is ubiquitously expressed, while expression of HIF-2α seems to be restricted to certain cell types including endothelial cells, hepatocytes, and glial cells (66). Activation of HIF is dependent upon stabilization of the oxygen-sensitive α subunit and its subsequent translocation to the nucleus, where it forms a functional complex with HIF-1β and cofactors such as CBP/p300 (55, 65). Under normoxic conditions, iron- and oxygen-dependent hydoxylation of specific proline residues within HIF-α is required for its binding to pVHL and subsequent ubiquitination which in turn results in its proteasomal degradation (12). Therefore, the loss of pVHL function, through stabilization of HIF-α, leads to constitutively active HIF, an effect that can be used to overexpress HIF experimentally (11, 19).

Functional studies of mice have shown that germ line inactivation of either *Vhlh* (gene symbol for murine *VHL*) or *Hif-1*α results in embryonic lethality (15, 26, 47), indicating that tight regulation of Hif-1-mediated adaptive responses to hypoxia are crucial for normal embryonic development and tissue function. Strongly dependent on genetic background, Hif-2α knockout mice, on the other hand, can survive into adulthood but display defects in their ability to efficiently scavenge reactive oxygen species (53).

Recent reports have shown that hypoxia seems to play an important role in T-cell development and function (5, 35), suggesting that pVHL and HIF may have a critical function during thymic development. During this process, T cells follow a specific sequence of defined maturation steps. Thymocytes lacking CD4 and CD8 surface antigens (double-negative [DN] cells) mature to thymocytes expressing both CD4 and CD8 surface antigens (double-positive [DP] cells). DP cells represent the largest thymocyte subset (~80%) and initiate expression of a fully functional αβ T-cell receptor (TCR) and then undergo selection on the basis of signal strength received through this receptor. The majority of DP cells die by programmed cell death, but a small proportion is positively selected for maturation and migrates into the periphery as single-positive (SP) cells, expressing either CD4 or CD8 surface antigen (54). The molecules and signaling cascades that underlie programmed cell death in thymocytes have been and still are subject to intense investigation (42, 45).

* Corresponding author. Mailing address: Department of Medicine, 700 Clinical Research Building, 415 Curie Blvd., Philadelphia, PA 19104-6144. Phone: (215) 573-1830. Fax: (215) 898-0189. E-mail: vhaase@mail.med.upenn.edu.

‡ M.P.B. and A.K.N. contributed equally to this work.

† Supplemental material for this article may be found at http://mcb.asm.org/.

TABLE 1. Primers used in this study

Target	Primers	Product size (bp)	Cycle no.
β-Actin	Forward 5′-ACTGGGACGACATGGAGAAG-3′ Reverse 5′-GGCGTGAGGGAGAGCATAG-3′	290	19
Bax	Forward 5′-ATCGAGCAGGGAGGATGG-3′ Reverse 5′-GGTCCCGAAGTAGGAGAGG-3′	404	24
Bnip3	Forward 5′-ACCTCGCTCCCAGACACC-3′ Reverse 5′-CAAATAACACACATAGTGCAAACACC-3′	495	26
Hif-1α	Forward 5′-GAGTTCTGAACGTCGAAAAG-3′ Reverse 5′-CTCACACGTAAATAACTGATGG-3′	171	26
Hif-2α	Forward 5′-GGACGCTCTGCCTATGAGTT-3′ Reverse 5′-GGCTCCTCCTTCAGTTTGG-3′	371	26
Pgk	Forward 5′-CAAACAACCAAAGGATCAAGG-3′ Reverse 5′-CCCAAGATAGCCAGGAAGG-3′	535	21
Vegf	Forward 5′-GAGACCCTGGTGGACATCTTC-3′ Reverse 5′-ATTTACACGTCTGCGGATCTTG-3′	394	30
Vhlh	Forward 5′-CTCAGGTCATCTTCTGCAACC-3′ Reverse 5′-TCCTTCAAGGCTCCTCTTCC-3′	438	26

We have used Cre-*loxP*-mediated recombination to gain insight into the role of pVHL during thymic development by generating mice that are either deficient for *Vhlh* alone or that lack both *Vhlh* and *Hif-1α* in thymocytes. Here, we show that *Vhlh* gene deletion in thymocytes results in increased Hif-1 transcriptional activity leading to increased apoptosis, and we propose that Hif-1 exerts its proapoptotic effect via a caspase-8-dependent mechanism.

MATERIALS AND METHODS

Generation and genotyping of mice. The generation of mice carrying *Vhlh* or *Hif-1α* 2-*lox* alleles has been described elsewhere previously (19, 48). Mice expressing a human BCL-2 transgene (Emu-*bcl-2-25* [58]) were obtained from the Jackson Laboratories (stock number 002320). Lck-Cre transgenic mice were a gift from Christopher Wilson, University of Washington (33). Thymus-specific *Vhlh* and *Hif-1α* mutants were of mixed genetic background (BALB/c, 129Sv/J, and C57BL/6). All procedures involving mice were performed according to National Institutes of Health guidelines for use and care of live animals and approved by the University of Pennsylvania Institutional Animal Care and Use Committee.

The following primers were used to detect 1-*lox* and 2-*lox* alleles of *Vhlh*: FwdI (5′-CTGGTACCCACGAAACTGTC-3′), FwdII (5′-CTAGGCACCGAGCTTAGAGGTTTGCG-3′), and Rev primer (5′-CTGACTTCCACTGATGCTTGTCACAG-3′). The *Vhlh* 2-*lox* allele was identified as a ~460-bp band, the 1-*lox* allele was detected as a ~260-bp band, and the wild-type allele was detected as a ~290-bp band. *Hif-1α* 1-*lox* and 2-*lox* alleles were detected with following primers: Fwd1 (5′-TTGGGGATGAAAACATCTGC-3′), Fwd2 (5′-GCAGTTAAGAGCACTAGTTG-3′), and Rev (5′-GGAGCTATCTCTCTAGACC-3′). The wild-type allele was identified as a ~240-bp band, the 2-*lox* allele was detected as a ~260-bp band, and 1-*lox* allele was detected as a ~270-bp band.

DNA isolation and Southern blotting. DNA from mouse tails and thymocytes was isolated according to the method described by Laird et al. (31) and used for PCR or Southern analysis. For Southern blot analysis, 10 to 20 μg of total DNA was digested with NcoI and size fractionated on a 0.7% agarose gel and then transferred to a nylon membrane by using an alkaline transfer method (51). The membrane was probed with a 200-bp 5′ NdeI-ApaI *Vhlh* probe as previously described (19).

RNA analysis. Total RNA from flow-sorted DN, DP, or SP thymocytes or total thymocytes was prepared with Trizol reagent (Invitrogen) according to the manufacturer's guidelines. Northern blot analysis was performed as described previously (19). Probes for *Pgk*, *Bnip3*, and *LdhA* were generated by reverse transcription-PCR (RT-PCR) from mouse thymus cDNA by using the primers described in Table 1. RNase protection analysis was performed by using a RiboQuant RNase protection assay kit (PharMingen) with mAng-1 multiprobe template sets.

RT-PCR. cDNA was synthesized from 200 ng to 1 μg of total RNA from sorted thymocyte subsets with a SuperScript first-strand synthesis system for RT-PCR (Invitrogen). Two microliters of cDNA was subjected to PCR amplification with gene-specific primers described in Table 1. The following thermal cycling profile was used: a denaturation step at 95°C for 2 min followed by cycles consisting of a denaturation step at 95°C for 30 s, an annealing step at 56°C for 35 s, and an extension step at 72°C for 1 min, including a final extension step at 72°C for 7 min.

Protein preparation and Western blot analysis. Thymocytes were lysed in buffer containing 50 mM Tris-HCl (pH 8.0), 1% Nonidet P-40, 150 mM NaCl, 5 mM EDTA, 1 μg of aprotinin/ml, 50 μg of phenylmethylsulfonyl fluoride/ml, and complete protease inhibitor cocktail (Roche). Fifty-microgram samples were size separated by sodium dodecyl sulfate–10 or 15% polyacrylamide gel electrophoresis and transferred to nitrocellulose membranes (Amersham Pharmacia Biotech, Piscataway, N.J.). After incubation with either anti-Bcl-X antibody (Transduction Laboratories), anti-human BCL-2 (Upstate), or anti-caspase 3 antibody (Cell Signaling), blots were washed and incubated with horseradish peroxidase-conjugated secondary antibody (Amersham Pharmacia Biotech) and developed with standard ECL reagent (Amersham Pharmacia Biotech) according to the manufacturer's instructions.

For detection of Hif-1α and Hif-2α, cytoplasmic and nuclear extracts were prepared as described previously (6). Thirty micrograms of either cytoplasmic or nuclear protein extract was size separated by 3 to 8% gradient SDS-PAGE (Invitrogen) and analyzed by Western blotting with rabbit anti-murine Hif-1α antiserum (Cayman) or rabbit anti-Hif-2α antiserum (Novus Biologicals).

EMSA. Nuclear and cytoplasmic protein isolation and electrophoretic mobility shift assay (EMSA) were performed by using erythropoietin-hypoxia response elements (EPO-HRE) as described previously (6).

Fluorescence-activated cell sorter (FACS) analysis. Thymocytes from 5- to 6-week-old mice were counted and stained with fluorochrome-conjugated monoclonal antibodies (Pharmingen) by using standard procedures. Acquisition was performed with a FACS Calibur (BD Biosciences).

Apoptosis and viability assays. The apoptosis DNA ladder assay was performed as follows. DNA from thymocytes was isolated with an apoptosis DNA ladder kit (Roche). Four micrograms of DNA was size fractioned by 1% agarose gel electrophoresis and stained with ethidium bromide. DNA bands were visualized by UV illumination and photographed by using a gel documentation system from Alpha Innotech.

7-AAD viability assay. A total of 10^6 trypan blue-negative thymocytes were plated in 48-well culture plates containing RPMI 1640 medium supplemented with 10% FBS. Samples were stained with 7-aminoactinomycin D (7-AAD; Viaprobe; Pharmingen) and analyzed by FACS. Data were expressed as percentages of the initial viable population. In addition to FACS staining with 7-AAD, viability was also evaluated manually by trypan blue exclusion using a hemocytometer. For caspase inhibition studies, caspase 8 inhibitor IETD-fmk, broad-spectrum caspase inhibitor z-VAD-fmk, granzyme B inhibitor zAAD-cmk, and caspase 9 inhibitor zLEHD-fmk were purchased from Calbiochem. Cell viability was analyzed after 24 h by 7-AAD staining.

JC-1/TOPRO-3 staining. Thymocytes were cultured as described above and harvested at the indicated times. Cells were washed and resuspended in 1 ml of phosphate-buffered saline and stained with 1 μg of JC-1 (Molecular Probes)/ml for 30 min at 37°C to examine mitochondrial membrane potential. To stain for plasma membrane integrity, TOPRO-3 (Molecular Probes) was added at 1 μM, 10 min prior to acquisition. Data were acquired by using a FACS Calibur and were presented as JC-1 multimer versus TOPRO-3 fluorescence.

TUNEL immunofluorescence microscopy. Frozen sections of thymic tissue were air dried and fixed in 4% paraformaldehyde. Staining for terminal deoxynucleotidyltransferase-mediated dUTP-biotin nick end labeling (TUNEL)-positive nuclei was carried out with an in situ cell death detection kit (Roche) according to the manufacturer's instructions. TUNEL-positive nuclei were visualized by using a Nikon E600 fluorescent microscope equipped with IP Lab image analysis software (Scanalytics Corp.).

Caspase 8 enzymatic activity colorimetric assay. Caspase 8 enzymatic activity was evaluated with a colorimetric assay kit (R&D Systems) according to the manufacturer's instructions. The cleavage of synthetic caspase 8 substrate IETD-pNA was detected spectrophotometrically by the formation of pNA.

Lectin staining of endothelial cells. Animals were anesthetized with tribromoethanol (Avertin) and infused via the inferior vena cava with a 400-μg/ml solution of fluorescein isothiocyanate (FITC)-labeled *Lycopersicon esculentum* lectin (Vector Labs) for 5 min. Paraffin sections were examined with a confocal laser microscope (LSM 410; Zeiss).

RESULTS

Generation of mice that lack *Vhlh* in thymocytes. Inactivation of *Vhlh* in the mouse germ line results in embryonic lethality from a lack of placental vasculogenesis (15) and precludes the analysis of *Vhlh* gene function in the adult by conventional gene targeting methods. In order to overcome this problem with embryonic lethality, we have generated a conditional *Vhlh* 2-*lox* allele (19). In this allele, the *Vhlh* promoter and exon 1 are flanked by *loxP* sites (Fig. 1A) and can be deleted by Cre-mediated recombination to generate a *Vhlh* null allele (1-*lox* allele). For the inactivation of *Vhlh* in thymocytes, transgenic mice expressing Cre recombinase under the control of the proximal Lck promoter (33) were bred to mice homozygous for the *Vhlh* 2-*lox* allele ($Vhlh^{2lox/2lox}$) or heterozygous for the *Vhlh* 2-*lox* and *Vhlh* 1-*lox* alleles ($Vhlh^{2lox/1lox}$). Most studies presented here were performed with $Vhlh^{2lox/2lox}$ Lck-Cre mice. Since results were similar to those obtained with $Vhlh^{2lox/1^{lox}}$ Lck-Cre mice, we hereafter refer to these mice collectively as $Vhlh^{-/-}$ mice. Cre-negative, $Vhlh^{2lox/2lox}$ littermates were used as controls. $Vhlh^{-/-}$ mice developed normally, were fertile, and had a normal life span.

Efficient developmental stage-specific inactivation and increased Hif target gene expression in $Vhlh^{-/-}$ mice. The expression of CD4 and CD8 surface markers divides thymocytes into three major cellular subtypes (54). In the DN stage, thymocytes are selected for their ability to recombine and express an in-frame TCR β chain. Selected clones expand and enter the DP stage. DP thymocytes rearrange their TCR α chain and undergo a second round of selection based on the specificity of the mature α/β TCR heterodimer for self-antigen plus major histocompatibility complex. As a result of this process, a relatively small fraction of DP thymocytes mature to either $CD4^+$ or $CD8^+$ cells and then emigrate to peripheral lymphoid organs as naive T cells. Thymocytes from $Vhlh^{-/-}$ mice showed greater than 90% recombination of the *Vhlh* 2-*lox* allele as determined by Southern blot analysis and genomic PCR (Fig. 1B and C). Only the 1-*lox* allele was clearly detectable in DN and DP thymocytes by PCR, suggesting virtually complete recombination of the 2-*lox* allele (Fig. 1C, lanes 3, 7, and 9). Higher levels of nonrecombined *Vhlh* were detected in SP thymocytes as well as in FACS-sorted peripheral T cells from spleen (PT) (Fig. 1C, lanes 14 and 16), indicating the presence of T cells derived from thymocytes with an incomplete deletion of *Vhlh*.

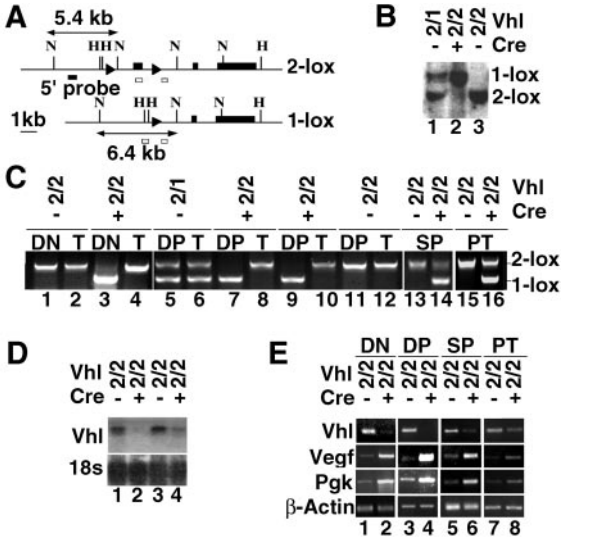

FIG. 1. Generation of mice lacking *Vhlh* in thymocytes. (A) Genomic organization of *Vhlh* 2-*lox* and 1-*lox* alleles. *loxP* sites are represented by triangles, and *Vhlh* exons 1 to 3 are depicted as black boxes. Restriction digestion with NcoI yields fragments of 5.4 kb for the 2-*lox* allele and 6.4 kb for the 1-*lox* allele. Open boxes depict the position of genomic PCR primer annealing sites. Abbreviations for restriction sites: H, HindIII; N, NcoI. (B) Detection of 2-*lox* and 1-*lox* alleles in nonsorted thymocytes by Southern blot. Abbreviations for genotypes: 2, 2-*lox* allele; 1, 1-*lox* allele; +, presence of Lck-Cre; −, absence of Lck-Cre. (C) Detection of 2-*lox* and 1-*lox* alleles in thymic subsets of different genotypes (top) by genomic PCR. T, tail DNA. (D) Analysis of *Vhlh* mRNA expression in nonsorted thymocytes by Northern blot; 18S rRNA was used as the loading control. (E) Hif target gene expression by semiquantitative RT-PCR in FACS-sorted thymocyte subsets. β-Actin is used to normalize mRNA. Data are representative of three separate experiments. Abbreviations for genotypes are the same as those described above (B).

Northern analysis of total thymus RNA indicated a >80% reduction in *Vhlh* transcript levels compared to the control by densitometry (Fig. 1D). *Vhlh* mRNA in FACS-sorted $Vhlh^{-/-}$ DP thymocytes were practically undetectable by semiquantitative RT-PCR analysis, while traces of the transcript were found in $Vhlh^{-/-}$ DN thymocytes at the same cycle number (Fig. 1E, lanes 2 and 4). Interestingly, the relative level of *Vhlh* mRNA in $Vhlh^{-/-}$ SP and PT cells was much higher than that in DN or DP cells but still significantly reduced compared to those of the controls (Fig. 1E, lanes 6 and 8). These findings are consistent with the level of Cre-mediated recombination detected by genomic PCR.

Since pVHL is required for the degradation of oxygen-sen-

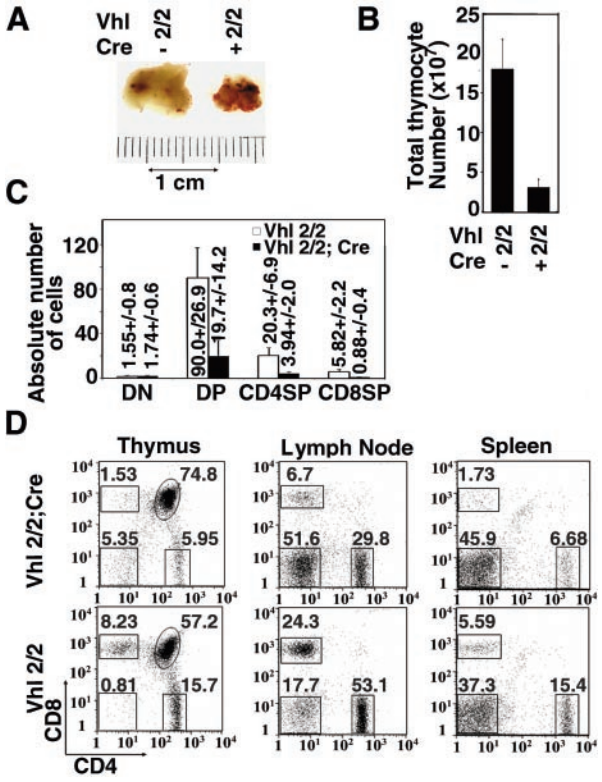

FIG. 2. *Vhlh* deletion in thymocytes results in small and highly vascularized thymi. (A) Gross photograph of mutant and control thymus. (B) Reduced thymic cellularity in mutant and control mice. Shown are mean values ± standard deviations (SD) for 14 mice. (C) Absolute numbers of thymocyte subtypes in millions. Note that similar numbers of DN cells are observed in mutant and control mice. Shown are mean values ± SD for five mice. (D) Representative FACS analysis of CD4 and CD8 surface expression in thymocytes and peripheral T cells from 5-week-old mice. Note the increase in the proportion of mutant DN thymocytes indicating normal absolute DN thymocyte numbers.

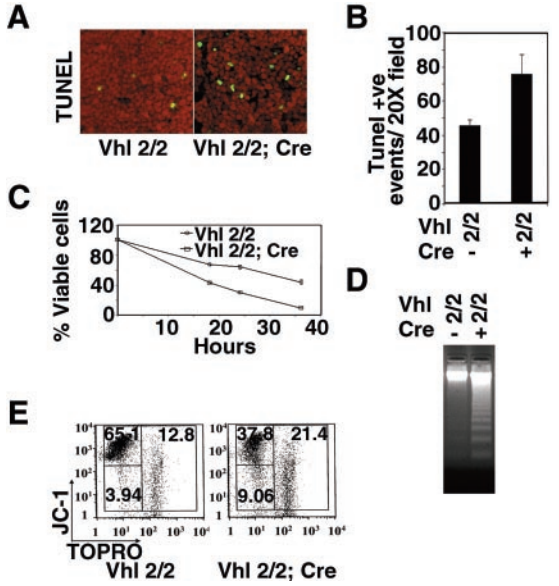

FIG. 3. Inactivation of *Vhlh* induces apoptosis in thymocytes. (A) Increased numbers of apoptotic cells and macrophages in *Vhlh* mutant thymi. Shown are cortical fields from TUNEL staining on frozen sections from mutant and control thymus. (B) Numerical representation of TUNEL-positive (Tunel +ve) cells. Values represent means ± SD for five randomly selected cortical fields (magnification, ×20). (C) Time course of neglect-induced thymocyte death. Shown are the percentages of viable cells in cultures of control and *Vhlh*-deficient thymocytes stained with viability marker 7-AAD. Mutant cells are represented by squares, and control cells are represented by circles. Shown are the mean values ± SD for six mice; individual experiments were carried out in triplicate. (D) Detection of DNA fragmentation in cultured thymocytes isolated from mutant and control mice. (E) Mitochondrial membrane potential and viability of thymocytes from cultures subjected to short-term neglect by staining with JC-1 and TOPRO-3. JC-1$^+$/TOPRO$^-$, viable cells with strong mitochondrial membrane potential ($\Delta\Psi_m$); JC-1$^-$/TOPRO$^-$, early apoptotic cells with loss of mitochondrial polarity and intact plasma membrane; JC-1$^-$/TOPRO$^+$, late apoptotic-necrotic compartment-containing cells with loss of $\Delta\Psi_m$ and membrane permeability. Note the increased numbers of JC-1$^-$/TOPRO$^-$ and JC-1$^-$/TOPRO$^+$ cells in *Vhlh* mutants. Shown are data representative of five independent experiments.

sitive Hif-α subunits by ubiquitination, we examined Hif target gene expression in FACS-sorted thymocyte subsets. We found a significant upregulation of representative Hif target genes (Fig. 1E) such as phosphoglycerate kinase (*Pgk*) and vascular endothelial growth factor (*Vegf*), the latter resulting in increased thymic vascularization manifested in a reddish, discolored thymus (Fig. 2A). As predicted, the degree of increase in Hif target gene induction was directly proportional to the level of Cre-mediated recombination and inversely proportional to *Vhlh* mRNA expression in theses cells.

Increased rates of apoptosis in *Vhlh*$^{-/-}$ thymocytes in vivo and in vitro. Based on macroscopic inspection, thymi from *Vhlh*$^{-/-}$ mice were small (Fig. 2A). This reduction in size is reflected in a 5- to 10-fold decrease in total thymocyte numbers (Fig. 2B). Analysis of thymocyte subsets by FACS showed that while absolute numbers in the DN compartment were comparable to those of the control, there was an ~80% reduction in total DP thymocyte numbers. Similarly, the percentages and numbers of SP thymocytes and peripheral T cells in spleen and lymph node were greatly reduced (Fig. 2C and D). We observed comparable reductions in thymic cellularity in *Vhlh*$^{-/-}$ mice of different ages, indicating that the thymic phenotype in *Vhlh*-deficient mice is not age restricted (data not shown).

To determine whether the reduction in thymocyte numbers was due to a block in proliferation or increased cell death, we used bromodeoxyuridine (BrdU) labeling to examine the rate of cell proliferation and TUNEL staining to evaluate apoptosis rates in *Vhlh*$^{-/-}$ thymi. *Vhlh*-deficient thymi did not exhibit significant differences in BrdU labeling (data not shown) of different thymocyte subsets compared to the control (data not shown); instead, we observed a statistically significant ($P < 0.05$) increase in TUNEL-positive nuclei (Fig. 3A and B), indicating enhanced apoptosis. The increased rates of apoptosis with no significant changes in BrdU labeling and a severe reduction in DP thymocyte numbers suggest that increased susceptibility of DP thymocytes to apoptosis rather than a problem with DN maturation or cell proliferation may have resulted in the severe decrease of thymocyte numbers in *Vhlh*$^{-/-}$ thymi.

In order to exclude environmental effects on thymocyte vi-

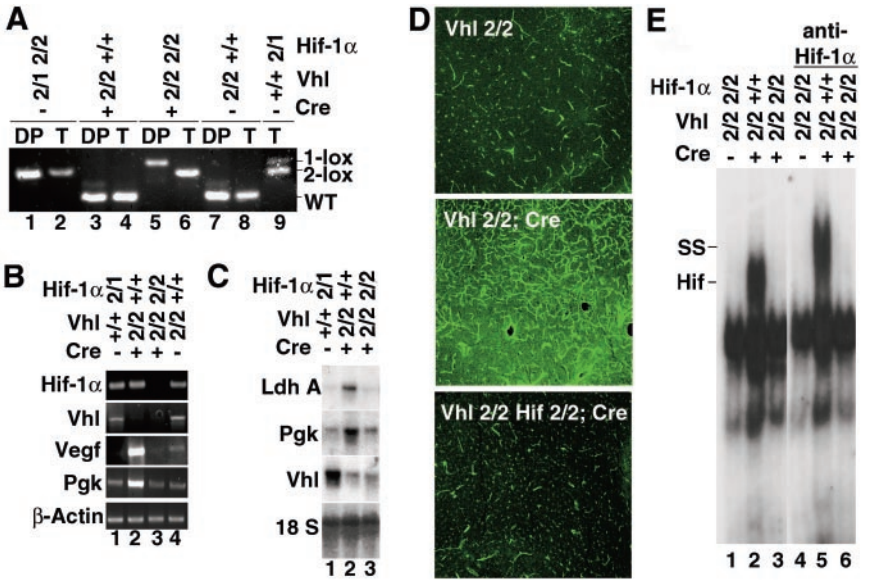

FIG. 4. Hif-1 dependence of target gene expression and angiogenic phenotype in *Vhlh* deficient thymi. (A) Highly efficient recombination of the *Hif-1*α 2-*lox* allele in *Vhlh*$^{-/-}$ DP thymocytes mediated by Lck-Cre. DP, FACS-sorted DP thymocytes; T, tail DNA from the same mouse. Abbreviations for genotypes: 2, 2-*lox* allele; 1, 1-*lox* allele; +, respective wild-type (WT) allele. Bands representing *Hif-1*α 2-*lox*, *Hif-1*α 1-*lox*, and wild-type alleles are identified on the right. (B and C) Inactivation of *Hif-1*α in *Vhlh*-deficient thymocytes suppresses transcription of Hif target genes completely. Shown are mRNA expression levels of *Vhlh* and classic Hif target genes *LdhA* and *Pgk* in nonsorted total thymocytes by Northern blot (18S rRNA is shown as loading control) and results from semiquantitative RT-PCR studies with FACS-sorted DP cells. Note that the reduction of *Vhlh* mRNA levels is similar in both the *Vhlh* and the *Vhlh*/*Hif-1* double mutant. (D) Suppression of increased microvascular density in *Vhlh*/*Hif-1* double-deficient thymi. Paraffin sections of thymi from control, *Vhlh* mutant, and *Vhlh*/*Hif-1* double mutant mice injected with endothelial cell-specific FITC-conjugated tomato lectin are shown. Sections were analyzed with confocal laser microscopy. (E) Hif binding activity to EPO-HRE in *Vhlh*-deficient thymocytes is suppressed by *Hif-1*α deletion. Shown are the control, the *Vhlh* mutant, and the *Vhlh*/*Hif-1* double mutant. SS indicates a supershift of Hif-1-containing complexes with a Hif-1α monoclonal antibody.

ability and apoptosis, we examined *Vhlh*-deficient thymocytes in vitro. For these studies, single-cell suspensions of thymocytes were cultured in RPMI 1640 medium supplemented with 10% fetal calf serum. Cell purity was confirmed by FACS (>98% were Thy1.1 positive). In culture, *Vhlh*$^{-/-}$ thymocytes exhibited greater than twofold accelerated death compared to controls when examined by FACS with 7-AAD staining (Fig. 3C). DNA laddering was enhanced significantly by 16 h of culture (Fig. 3D).

We next determined the degree of apoptosis with JC-1 (57), a fluorescent compound that measures mitochondrial membrane potential, in conjunction with TOPRO-3, a commonly used viability marker (63). JC-1 enters charged mitochondrial membranes, where it multimerizes and exhibits red fluorescence. Staining with TOPRO-3 is excluded from cells possessing intact plasma membranes. A loss of mitochondrial membrane potential in the absence of plasma membrane permeability is a classic feature of apoptotic cells, whereas plasma membrane integrity is typically lost in necrotic or late apoptotic cells, resulting in positive staining by TOPRO-3. After 24 h in culture, *Vhlh*$^{-/-}$ thymocytes showed an at least a two- to threefold increase in the percentage of cells undergoing apoptosis as well as an increase in the late apoptotic-necrotic population (Fig. 3E). Staining with Annexin-V (64) and TOPRO-3 gave similar results (data not shown). These data suggest that *Vhlh*$^{-/-}$ thymocytes are more susceptible to apoptosis in vitro. In addition, bone marrow from *Vhlh*$^{-/-}$ mice was used to reconstitute lethally irradiated mice. Thymi of these chimeric mice showed similar reductions in thymocyte numbers and increased apoptosis (data not shown). This finding suggests that the observed increase in apoptosis in *Vhlh*$^{-/-}$ thymocytes is cell intrinsic.

Hif-1 is the key mediator of Hif target gene expression in *Vhlh*-deficient thymocytes. Increased transcriptional activity of Hif-1 has been shown to promote angiogenesis as well as apoptosis (recently reviewed by Harris [21] and Pugh and Ratcliffe [44]). In order to examine the role of Hif-1 in the development of the thymic phenotype associated with *Vhlh* gene deletion, we generated mice that lack both *Vhlh* and Hif-1 in thymocytes.

For this purpose, we crossed the *Hif-1*α 2-*lox* allele (48) into the *Vhlh* 2-*lox* background. In the *Hif-1*α 2-*lox* allele, *Hif-1*α exon 2, encoding the basic helix-loop-helix domain, is flanked by *loxP* sites and deleted by Cre-mediated recombination. Since this out-of-frame deletion results in the absence of Hif-1 heterodimers, Hif-1α-deficient cells or mice are hereafter referred to as Hif-1 deficient. Offspring carrying floxed alleles for both *Vhlh* and *Hif-1*α were then mated with Lck-Cre transgenic mice to generate thymocyte-specific *Vhlh*/*Hif-1*α double-knockout mice. Recombination efficiency was analyzed by genomic PCR and RT-PCR. In *Vhlh*$^{2lox/2lox}$, *Hif-1*α$^{2lox/2lox}$, Lck-Cre mice (hereafter referred to as *Vhlh*/*Hif-1*$^{-/-}$ mice), all floxed alleles were recombined with high efficiency (Fig. 4A). Semiquantitative RT-PCR analysis of Hif target gene expression in *Vhlh*/*Hif-1*$^{-/-}$ total and DP thymocytes showed virtually complete suppression of *Pgk*, lactate dehydrogenase A (*LdhA*),

and *Vegf* mRNA levels compared to *Vhlh*$^{-/-}$ thymocytes while the reduction of *Vhlh* mRNA was similar (Fig. 4B and C) (see Fig. S1 in the supplemental material). As a result of normalized *Vegf* mRNA levels, the increase in thymic vascularization found in *Vhlh*$^{-/-}$ mutants was completely suppressed in *Vhlh*/*Hif-1*$^{-/-}$ double mutants as demonstrated by staining with endothelial cell-specific FITC-labeled tomato lectin (Fig. 4D). Consistent with this finding is the return of *Flt-1*, endoglin, and *CD31* mRNA to baseline levels in *Vhlh*/*Hif-1*$^{-/-}$ double mutants compared to the *Vhlh*$^{-/-}$ mutant and the control (Fig. S1 in the supplemental material). Interestingly, we could not detect Hif-2α protein in the nuclear fraction of *Vhlh*$^{-/-}$ thymocytes despite the fact that semiquantitative RT-PCR analysis indicated increased Hif-1-dependent *Hif-2*α transcription (Fig. S2 in the supplemental material). This finding together with the absence of EPO-HRE binding by EMSA in *Vhlh*/*Hif-1*$^{-/-}$ thymocytes (Fig. 4E) suggest that Hif-1 is the main regulator of Hif target gene expression in *Vhlh*$^{-/-}$ thymocytes and that Hif-2 does not seem to play a significant role in the transcriptional regulation of Hif target genes examined here.

Conditional disruption of *Hif-1*α in *Vhlh*$^{-/-}$ thymocytes restores thymic cellularity and improves thymocyte viability in vitro. Total thymocyte numbers in *Vhlh*/*Hif-1*$^{-/-}$ mice were significantly increased (~1.5- to 1.8-fold reduction in *Vhlh*/*Hif-1*$^{-/-}$ thymi compared to a ~5- to 10-fold reduction in *Vhlh*$^{-/-}$ thymi) but lower than those in wild-type mice (Fig. 5A), while a similar decrease in thymocyte numbers was found in mice that were Hif-1 deficient but *Vhlh* competent, indicating that the absence of Hif-1 alone has a negative effect on thymocyte development (Fig. 5A). Figure 5B shows a representative litter from a cross that generated wild-type and *Vhlh*$^{-/-}$ mice which were either *Hif-1*α competent or lacked one or both copies of *Hif-1*α. It is interesting that total thymocyte numbers in *Vhlh*$^{-/-}$ mice lacking only one copy of *Hif-1*α were already significantly increased compared to those of *Vhlh*$^{-/-}$ mutants (Fig. 5A and B). These findings suggest that *Hif-1*α gene deletion improves *Vhlh*$^{-/-}$ thymocyte cell survival in a gene dose-dependent manner. *Vhlh*/*Hif-1*$^{-/-}$ thymocyte viability in culture was improved as shown by FACS analysis with 7-AAD, and fewer JC-1- and TOPRO-3-negative apoptotic cells were present compared to *Vhlh*-deficient cells (Fig. 5D and E). This observation was also reflected in a reduction of DNA laddering in *Vhlh*/*Hif-1*$^{-/-}$ thymocytes (Fig. 5F). Our findings suggest that impaired survival of *Vhlh*$^{-/-}$ thymocytes in vivo and in vitro is Hif-1 dependent.

Increased caspase 8 activity results in impaired survival of *Vhlh*$^{-/-}$ thymocytes. Our in vivo and in vitro studies with *Vhlh*/*Hif-1*$^{-/-}$ thymocytes clearly suggest that Hif-1 plays a key role in mediating the proapoptotic effects of *Vhlh* gene deletion. This notion is supported by direct and indirect evidence that increased Hif-1 activity under hypoxic conditions can promote apoptosis through mechanisms involving both classic caspase 3-dependent intrinsic and extrinsic pathways and nonclassic Bnip3 (4, 7, 21).

In order to gain insight into the mechanisms that result in increased apoptosis in *Vhlh*$^{-/-}$ thymocytes, we first investigated whether the expression levels of Bcl-X_L and Bcl-2, both of which are critical for thymocyte survival and belong to the intrinsic apoptosis pathway (reviewed by Gross et al. [17]), were altered. While the expression of Bcl-2 is normally low in

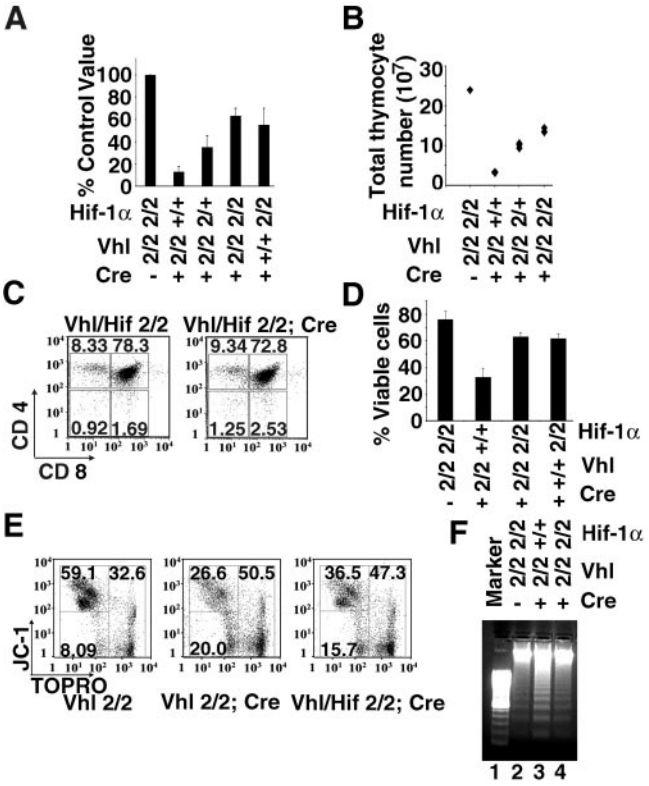

FIG. 5. *Hif-1*α gene deletion improves thymic cellularity and thymocyte viability in vitro. (A) Thymic cellularity in *Vhlh*/*Hif-1* double mutants. Shown is the decrease in total thymocyte numbers expressed as a percentage of littermate control values. Numbers represent mean values ± SD for 12 to 16 mice. Abbreviations for genotypes: 2, 2-*lox* allele; 1, 1-*lox* allele; +, respective wild-type allele. (B) Actual total thymocyte numbers in a representative litter (parents were both heterozygous for the *Hif-1*α 2-*lox* allele). Note that thymic cellularity in *Vhlh*$^{-/-}$ thymi which lack one copy of *Hif-1*α is increased but does not reach the level of *Vhlh*/*Hif-1*α double-deficient thymi. (C) Representative FACS analysis of CD4 and CD8 surface expression in thymocytes from 5-week-old mice. (D) 7-AAD viability stain of *Vhlh*/*Hif-1* double-deficient, *Vhlh*-deficient, *Hif-1*-deficient, and control thymocytes (24 h of culture). (E) Mitochondrial membrane potential and viability of control, *Vhlh*-deficient, and *Vhlh*/*Hif-1*α double-deficient thymocytes from 24-h cultures by staining with JC-1 and TOPRO-3. (F) Apoptosis in thymocyte cultures from *Vhlh*-deficient, *Vhlh*/*Hif-1* double-deficient, and control mice by DNA ladder assay.

DP cells and increases in SP cells (16), Bcl-X_L is predominantly expressed in DP thymocytes (34). Transgenic studies have suggested that both factors appear to be interchangeable on a functional level (8). In *Vhlh*$^{-/-}$ mice, Bcl-X_L mRNA and protein levels were decreased in FACS-sorted DPs but were not changed in *Vhlh*/*Hif-1*$^{-/-}$ thymocytes (Fig. 6A), while Bcl-2 protein levels in DP thymocytes did not change (data not shown). Protein levels for Bim, another important Bcl-2 family proapoptotic factor in thymocytes (3), were not changed (data not shown), while Bax mRNA was elevated (Fig. 6B). Although our data suggest that the balance of pro- versus anti-apoptotic Bcl-2 family gene expression in *Vhlh*$^{-/-}$ DP thymocytes is shifted towards a Hif-1-dependent expression pattern which favors apoptosis, transgenic expression of BCL-2 or BCL-X_L (Fig. 6D and data not shown) did not significantly improve survival of *Vhlh*-deficient thymocytes. Western blot

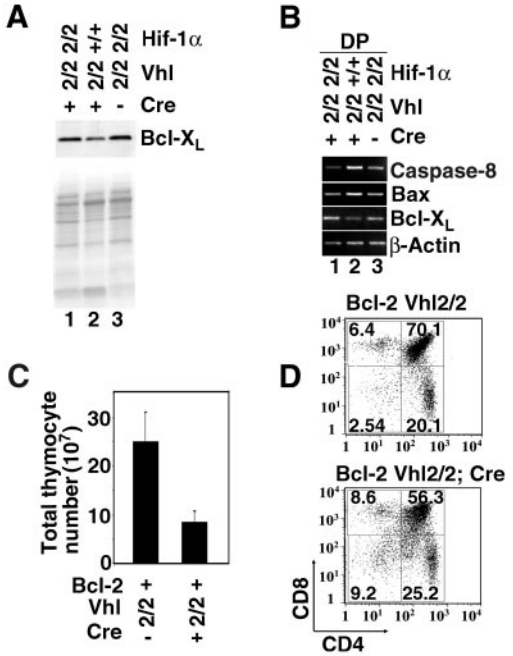

FIG. 6. Hif-1 dependence of apoptosis gene expression in *Vhlh*$^{-/-}$ thymocytes. (A) Normalization of Bcl-X_L protein levels in *Vhlh*/*Hif-1* double-deficient thymocytes. (B) Normalization of caspase 8, *Bax*, and *Bcl-X_L* mRNA expression in *Vhlh*/*Hif-1* double-deficient DP thymocytes by RT-PCR. (C) Thymic cellularity in *Vhlh*-deficient animals and control mice expressing a human *BCL-2* transgene. Shown are mean values ± SD for 12 mice. Abbreviations of genotypes are as described in the legends of Fig. 4 and 5. (D) FACS analysis of CD4 and CD8 surface expression in *BCL-2* transgenic *Vhlh*$^{-/-}$ and control thymocytes. Shown is one representative FACS study of four studies performed.

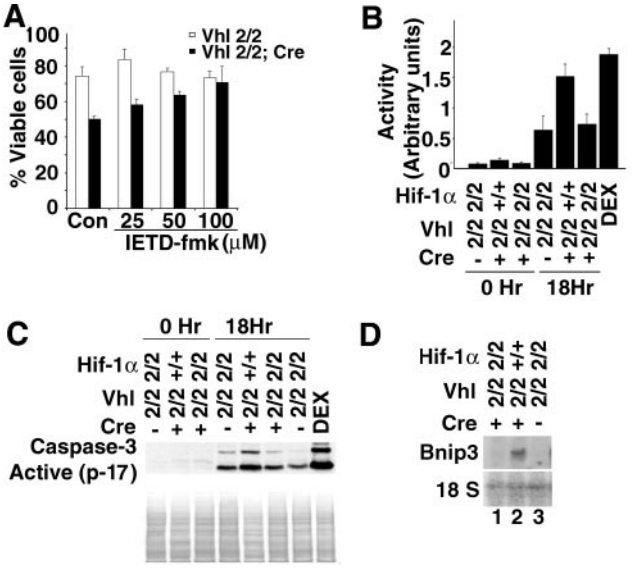

FIG. 7. *Vhlh* deletion induces thymocyte death through the caspase 8-dependent pathway. (A) Dose-dependent rescue of thymocyte viability with caspase 8 inhibitor IETD-fmk. Shown are the percentages of viable cells in cultures of control and *Vhlh*-deficient thymocytes treated for 24 h with different concentrations of IETD-fmk and stained with viability marker 7-AAD. Dimethyl sulfoxide-treated cells were used as the control (Con). Shown are the mean values ± SD for three mice; individual experiments were carried out in triplicate. (B) Enzyme activity assay of caspase 8 in cultured *Vhlh*-deficient, *Vhlh*/*Hif-1* double-deficient, and control thymocytes after 0 and 18 h. Dexamethasone (100 nM)-treated thymocytes were used as positive controls (DEX). Shown are the mean values ± SD for four mice; individual experiments were carried out in duplicate. (C) Protein levels of cleaved caspase 3 in cultured *Vhlh*-deficient, *Vhlh*/*Hif-1* double-deficient, and control thymocytes after 0 and 18 h by Western blot analysis. Dexamethasone (100 nM)-treated thymocytes were used as positive controls. Staining with Ponceau S is shown to demonstrate equal loading. (D) Induction of *Bnip3* mRNA in *Vhlh*-deficient thymocytes but not in *Vhlh*/*Hif-1*-deficient thymocytes. Total thymus RNA was analyzed by Northern blot. 18S rRNA was used as the loading control.

analysis confirmed that BCL-2 transgene expression was not affected by *Vhlh* deficiency (Fig. S3 in the supplemental material). Moreover, inhibition of caspase 9, an essential throughput element in the mitochondrially gated pathway of apoptosis, had no effect on *Vhlh*$^{-/-}$ thymocyte survival (Fig. S4 in the supplemental data). This finding suggests that Bcl-2-dependent apoptosis pathways (intrinsic apoptosis pathway) do not play a critical role in Hif-1-induced thymocyte death.

We next investigated whether key mediators of the extrinsic pathway could be responsible for Hif-1-driven thymocyte death in a *Vhlh*$^{-/-}$ background. In the extrinsic or death receptor (DR) pathway, ligand binding to the DR (e.g., TNFR60, Fas/Apo1, or TRAIL-R/Apo2) leads to the recruitment and activation of caspase 8 through specific adaptor molecules such as the Fas-associated death domain protein (FADD) (10, 61). Besides ligand-induced receptor activation, the DR pathway can also be induced by UV irradiation, DNA damage, or cell detachment in a ligand-independent fashion (39, 49, 52, 56). DR and FADD activation of caspase 8 leads to cleavage and induction of effector caspase 3, resulting in cell death.

In *Vhlh*-deficient thymocytes, we found a Hif-1-dependent increase in caspase 8 mRNA (Fig. 6) and used specific small peptide inhibitors to examine whether caspase-specific inhibition was effective in improving survival of *Vhlh*$^{-/-}$ thymocytes. Incubation of *Vhlh*$^{-/-}$ thymocytes with caspase 8-specific inhibitor IETD-fmk restored the percentage of viable cells to control values (Fig. 7A). Since IETD-fmk can inhibit both caspase 8 and granzyme B, a specific inhibitor for granzyme B was used to address this possibility. We used zAAD-cmk, a specific inhibitor of granzyme B, and found that inhibition of granzyme B had no effect on *Vhlh*$^{-/-}$ thymocyte survival (Fig. S4 in the supplemental material) (60). This finding suggests that induction of caspase 8 enzymatic activity may have resulted in decreased survival of *Vhlh*$^{-/-}$ thymocytes. We next determined caspase 8 enzymatic activity with a colorimetric assay kit (R&D Systems). The quantity of chromogenic compound pNA, which is released from synthetic caspase 8 substrate IETD-pNA, was used as an index of caspase 8 enzymatic activity. Enzymatic activity was increased by at least twofold in *Vhlh*$^{-/-}$ cells compared to that of the control, while caspase 8 enzymatic activity in *Vhlh*/*Hif-1* double-deficient thymocytes was not different from that of control cells. Our data suggest that caspase 8 enzymatic activity is increased in *Vhlh*$^{-/-}$ thymocytes and that its increase is Hif-1 dependent (Fig. 7B).

Since activated caspase 8 results in the induction of caspase 3, we measured caspase 3 enzymatic activity in control, *Vhlh*$^{-/-}$, and *Vhlh*/*Hif-1* double-deficient thymocytes. We found that caspase 3 enzymatic activity, as indicated by the

increase in cleaved caspase 3, paralleled the increase in caspase 8 enzymatic activity in $Vhlh^{-/-}$ cells (Fig. 7C).

Although the nonclassic proapoptotic gene *Bnip3* is strongly induced by Hif-1 (Fig. 7D), a complete rescue with inhibition of caspase 8 indicates that Bnip3 may not play a significant role in Hif-1-mediated thymocyte death. Taken together, our findings suggest that the loss of *Vhlh* in thymocytes results in a Hif-1-dependent increase in caspase 8 enzymatic activity resulting in increased apoptosis.

DISCUSSION

The role of hypoxia as a modifier of differentiation and the importance of HIF transcription factors in the regulation of normal embryonic development have been well demonstrated (1, 26, 37, 47). Previous reports have documented areas of local hypoxia in the normal thymus (20), suggesting that HIF-mediated adaptive responses to lowered oxygen levels may play an important role in thymic development and apoptosis. It is now well established that the VHL tumor suppressor (pVHL), which was initially identified as the protein mutated in patients with von Hippel-Lindau familial tumor syndrome (29, 32), is a global regulator of HIF-α subunit stability (24, 27, 38, 50) and operates in tissues that are normally not affected by the disease (11, 43). Experimental manipulations of pVHL can therefore be used to provide clues to HIF function in adult tissues or during development. Nevertheless, pVHL has other roles besides that of controlling HIF activity, for example, regulating fibronectin extracellular matrix assembly and microtubule stability (22, 41), which need to be taken into account when interpreting mouse phenotypes resulting from *Vhlh* gene deletion.

Here, we have investigated how inactivation of *Vhlh* in wild-type and *Hif-1*-deficient backgrounds affects thymic development, and we provide evidence for a critical role of the pVhl/Hif-1 pathway during thymocyte maturation. A 5- to 10-fold reduction in DP thymocyte numbers without any change in DN thymocyte numbers, normal distribution of DN subtypes, and no changes in BrdU labeling (data not shown) suggested that the reduction in total thymocyte numbers in *Vhlh*-deficient thymi was a result of decreased DP cell survival. Indeed, we found a ~2-fold increase in TUNEL-positive cells in vivo. Since apoptotic thymocytes are usually rapidly cleared by local macrophages (59), the degree of apoptosis in *Vhlh*-deficient thymi may be underrepresented by this figure. Since it is possible that the phenotype of $Vhlh^{-/-}$ thymi is much more complex and probably involves additional defects such as abnormal TCR signaling interfering with thymocyte selection, studies in our lab are under way to address these questions. Nevertheless, our in vivo and in vitro data showed a Hif-1-dependent increase in apoptosis as demonstrated by TUNEL staining, DNA laddering, the loss of mitochondrial membrane potential, and Annexin V staining, indicating that one of the underlying features of the $Vhlh^{-/-}$ phenotype is abnormal regulation of thymocyte programmed cell death.

Hif-1 has been shown to induce cell death either by stabilizing p53, through a Bnip3/Nix-dependent mechanism, or by altering the expression of Bcl-2 family members (7, 21). While we ruled out significant alterations in p53 levels as a cause of enhanced apoptosis (data not shown), we found a Hif-1-dependent decrease in Bcl-X_L, a well-established survival factor for DP thymocytes (34). Although we initially hypothesized that decreased Bcl-X_L might have played a significant role in the development of this phenotype, we observed only a minor improvement in cell survival by BCL-2 or BCL-X_L transgene expression in $Vhlh^{-/-}$ mice. When the strong antiapoptotic effect of BCL-2 on mitochondrion-dependent death is considered, our result argues that the proapoptotic phenotype in $Vhlh^{-/-}$ mice is not mediated by classic mitochondrion-dependent death mechanisms.

Our findings suggest that Hif-1 exerts its proapoptotic effect through a caspase 8-dependent mechanism, and it is interesting to speculate whether regional hypoxia in normal thymi can modulate thymocyte susceptibility to apoptosis by enhancing caspase 8 activity through an increase in Hif-1α expression. Caspase 8/FADD has been shown to play an important role in hypoxia-induced apoptosis, although a link to Hif had not been established. In primary cardiomyocytes, apoptosis induced by severe hypoxia can be prevented by use of caspase 8 inhibitor CrmA or a dominant-negative mutant of FADD (9, 18). Furthermore, in the presence of sufficient glucose, a caspase 8-dependent rather than a mitochondrion-dependent death mechanism seems to be active in Jurkat cells (36), and caspase 8-mediated apoptosis in DP thymocytes seems to be important for thymic maturation (28). Whether the increase in caspase 8 mRNA alone is sufficient or whether caspase 8 is activated by a ligand-dependent or -independent mechanism in $Vhlh^{-/-}$ thymocytes remains to be investigated. Both mechanisms are certainly a possibility, as VHL deficiency has been shown to increase tumor necrosis factor alpha secretion in renal carcinoma cells (13) and DR-independent activation of caspase 8, for example, can occur through the formation of a Hip-1/Hippi procaspase recruitment complex (14). The role of Bnip3 in Hif-1-mediated thymocyte apoptosis at this point remains unclear. It has been suggested that Bnip3 induces apoptosis through a nonclassic, caspase 3-independent mechanism (62). Our in vitro studies, however, suggest that Bnip3 does not play a significant role in thymocyte death induced by *Vhlh* gene deletion, which may be different under hypoxic conditions.

Thymocyte subset distribution in $Hif\text{-}1^{-/-}$ thymi obtained from $Rag\text{-}1^{-/-}$ chimeric mice was normal, while absolute numbers were not reported (30). We found that despite comparable thymocyte subset distribution, absolute numbers and viability in $Vhlh/Hif\text{-}1^{-/-}$ and $Hif\text{-}1^{-/-}$ mice were not completely normal (there was a mild to moderate decrease in absolute thymocyte numbers), suggesting that the loss of Hif-1 by itself may have a negative effect on thymic development. Efforts to understand reduced thymic cellularity in $Hif\text{-}1^{-/-}$ mice and whether genetic background may play a role are currently under way in our laboratory.

The second major target of pVHL-mediated ubiquitination is HIF-2α (38, 40). We have shown that the expression of Hif target genes such as *Vegf*, *Pgk*, *LdhA*, and others is increased in *Vhlh*-deficient thymocytes. Surprisingly, upregulation of these genes and Hif binding to EPO-HRE by EMSA were completely suppressed in *Vhlh*/*Hif-1*α double-deficient thymi, arguing that Hif-1, despite the presence of *Hif-2*α mRNA, must be the main effector of Hif-controlled gene expression in thymocytes. *Vegf*, for example, is a well-established Hif-2 target gene in *VHL*-deficient renal carcinoma cells and other cell

types (38) but is not upregulated in *Vhlh/Hif-1*$^{-/-}$ thymi, thus resulting in their normal vascularity.

To our knowledge, abnormal T-cell development or function has not been reported in patients with VHL disease or Chuvash polycythemia, a congenital form of polycythemia caused by a specific germ line mutation in the VHL gene (2). It is plausible that, according to Knudson's two-hit hypothesis (23, 46), inactivation of the remaining wild-type allele in thymocytes or T-cells may be a rare event in VHL patients or that most VHL-deficient thymocytes are eliminated because of increased susceptibility to apoptosis, therefore representing only a minor population in peripheral lymphoid tissues. However, investigations of T-cell function in patients with *VHL* germ line mutations may be warranted.

In summary, in this report, we demonstrate that proper regulation of Hif-1 transcriptional activity through pVhl is required for normal thymocyte development and we provide a link between constitutively active Hif-1 and caspase 8-mediated cell death. Our data suggest that Hif-1 may play an important role in regulating apoptosis during normal thymic development.

ACKNOWLEDGMENTS

This work was supported by a grant from the American Heart Association (0365342U) and in part by grants from the NIH (R03-DK-62060), the Charlotte Geyer Foundation, and seed money from the Department of Medicine, University of Pennsylvania (all to V.H.H.).

We are grateful to the members of the Morphology Core, in particular Gary Swain, Penn Center for Molecular Studies in Digestive and Liver Disease (P30-DK50306), for help with immunohistochemistry and image analysis. We thank Celeste Simon, Debra Higgins, and Erinn Bruno for critical reading of the manuscript.

REFERENCES

1. **Adelman, D. M., M. Gertsenstein, A. Nagy, M. C. Simon, and E. Maltepe.** 2000. Placental cell fates are regulated in vivo by HIF-mediated hypoxia responses. Genes Dev. **14:**3191–3203.
2. **Ang, S. O., H. Chen, K. Hirota, V. R. Gordeuk, J. Jelinek, Y. Guan, E. Liu, A. I. Sergueeva, G. Y. Miasnikova, D. Mole, P. H. Maxwell, D. W. Stockton, G. L. Semenza, and J. T. Prchal.** 2002. Disruption of oxygen homeostasis underlies congenital Chuvash polycythemia. Nat. Genet. **32:**614–621.
3. **Bouillet, P., D. Metcalf, D. C. Huang, D. M. Tarlinton, T. W. Kay, F. Kontgen, J. M. Adams, and A. Strasser.** 1999. Proapoptotic Bcl-2 relative Bim required for certain apoptotic responses, leukocyte homeostasis, and to preclude autoimmunity. Science **286:**1735–1738.
4. **Bruick, R. K.** 2000. Expression of the gene encoding the proapoptotic Nip3 protein is induced by hypoxia. Proc. Natl. Acad. Sci. USA **97:**9082–9087.
5. **Caldwell, C. C., H. Kojima, D. Lukashev, J. Armstrong, M. Farber, S. G. Apasov, and M. V. Sitkovsky.** 2001. Differential effects of physiologically relevant hypoxic conditions on T lymphocyte development and effector functions. J. Immunol. **167:**6140–6149.
6. **Camenisch, G., R. H. Wenger, and M. Gassmann.** 2002. DNA-binding activity of hypoxia-inducible factors (HIFs). Methods Mol. Biol. **196:**117–129.
7. **Carmeliet, P., Y. Dor, J. M. Herbert, D. Fukumura, K. Brusselmans, M. Dewerchin, M. Neeman, F. Bono, R. Abramovitch, P. Maxwell, C. J. Koch, P. Ratcliffe, L. Moons, R. K. Jain, D. Collen, E. Keshert, and E. Keshet.** 1998. Role of HIF-1α in hypoxia-mediated apoptosis, cell proliferation and tumour angiogenesis. Nature **394:**485–490.
8. **Chao, D. T., G. P. Linette, L. H. Boise, L. S. White, C. B. Thompson, and S. J. Korsmeyer.** 1995. Bcl-XL and Bcl-2 repress a common pathway of cell death. J. Exp. Med. **182:**821–828.
9. **Chao, W., Y. Shen, L. Li, and A. Rosenzweig.** 2002. Importance of FADD signaling in serum deprivation- and hypoxia-induced cardiomyocyte apoptosis. J. Biol. Chem. **277:**31639–31645.
10. **Chinnaiyan, A. M., K. O'Rourke, M. Tewari, and V. M. Dixit.** 1995. FADD, a novel death domain-containing protein, interacts with the death domain of Fas and initiates apoptosis. Cell **81:**505–512.
11. **Cramer, T., Y. Yamanishi, B. E. Clausen, I. Forster, R. Pawlinski, N. Mackman, V. H. Haase, R. Jaenisch, M. Corr, V. Nizet, G. S. Firestein, H. P. Gerber, N. Ferrara, and R. S. Johnson.** 2003. HIF-1α is essential for myeloid cell-mediated inflammation. Cell **112:**645–657.
12. **Epstein, A. C., J. M. Gleadle, L. A. McNeill, K. S. Hewitson, J. O'Rourke, D. R. Mole, M. Mukherji, E. Metzen, M. I. Wilson, A. Dhanda, Y. M. Tian, N. Masson, D. L. Hamilton, P. Jaakkola, R. Barstead, J. Hodgkin, P. H. Maxwell, C. W. Pugh, C. J. Schofield, and P. J. Ratcliffe.** 2001. *C. elegans* EGL-9 and mammalian homologs define a family of dioxygenases that regulate HIF by prolyl hydroxylation. Cell **107:**43–54.
13. **Galbán, S., J. Fan, J. L. Martindale, C. Cheadle, B. Hoffman, M. P. Woods, G. Temeles, J. Brieger, J. Decker, and M. Gorospe.** 2003. von Hippel-Lindau protein-mediated repression of tumor necrosis factor alpha translation revealed through use of cDNA arrays. Mol. Cell. Biol. **23:**2316–2328.
14. **Gervais, F. G., R. Singaraja, S. Xanthoudakis, C. A. Gutekunst, B. R. Leavitt, M. Metzler, A. S. Hackam, J. Tam, J. P. Vaillancourt, V. Houtzager, D. M. Rasper, S. Roy, M. R. Hayden, and D. W. Nicholson.** 2002. Recruitment and activation of caspase-8 by the Huntingtin-interacting protein Hip-1 and a novel partner Hippi. Nat. Cell Biol. **4:**95–105.
15. **Gnarra, J. R., J. M. Ward, F. D. Porter, J. R. Wagner, D. E. Devor, A. Grinberg, M. R. Emmert-Buck, H. Westphal, R. D. Klausner, and W. M. Linehan.** 1997. Defective placental vasculogenesis causes embryonic lethality in VHL-deficient mice. Proc. Natl. Acad. Sci. USA **94:**9102–9107.
16. **Gratiot-Deans, J., R. Merino, G. Nunez, and L. A. Turka.** 1994. Bcl-2 expression during T-cell development: early loss and late return occur at specific stages of commitment to differentiation and survival. Proc. Natl. Acad. Sci. USA **91:**10685–10689.
17. **Gross, A., J. M. McDonnell, and S. J. Korsmeyer.** 1999. BCL-2 family members and the mitochondria in apoptosis. Genes Dev. **13:**1899–1911.
18. **Gurevich, R. M., K. M. Regula, and L. A. Kirshenbaum.** 2001. Serpin protein CrmA suppresses hypoxia-mediated apoptosis of ventricular myocytes. Circulation **103:**1984–1991.
19. **Haase, V. H., J. N. Glickman, M. Socolovsky, and R. Jaenisch.** 2001. Vascular tumors in livers with targeted inactivation of the von Hippel-Lindau tumor suppressor. Proc. Natl. Acad. Sci. USA **98:**1583–1588.
20. **Hale, L. P., R. D. Braun, W. M. Gwinn, P. K. Greer, and M. W. Dewhirst.** 2002. Hypoxia in the thymus: role of oxygen tension in thymocyte survival. Am. J. Physiol. Heart Circ. Physiol. **282:**H1467–H1477.
21. **Harris, A. L.** 2002. Hypoxia—a key regulatory factor in tumour growth. Nat. Rev. Cancer **2:**38–47.
22. **Hergovich, A., J. Lisztwan, R. Barry, P. Ballschmieter, and W. Krek.** 2003. Regulation of microtubule stability by the von Hippel-Lindau tumour suppressor protein pVHL. Nat. Cell Biol. **5:**64–70.
23. **Herman, J. G., F. Latif, Y. Weng, M. I. Lerman, B. Zbar, S. Liu, D. Samid, D. S. Duan, J. R. Gnarra, W. M. Linehan, et al.** 1994. Silencing of the VHL tumor-suppressor gene by DNA methylation in renal carcinoma. Proc. Natl. Acad. Sci. USA **91:**9700–9704.
24. **Ivan, M., K. Kondo, H. Yang, W. Kim, J. Valiando, M. Ohh, A. Salic, J. M. Asara, W. S. Lane, and W. G. Kaelin, Jr.** 2001. HIFα targeted for VHL-mediated destruction by proline hydroxylation: implications for O_2 sensing. Science **292:**464–468.
25. **Iwai, K., K. Yamanaka, T. Kamura, N. Minato, R. C. Conaway, J. W. Conaway, R. D. Klausner, and A. Pause.** 1999. Identification of the von Hippel-Lindau tumor-suppressor protein as part of an active E3 ubiquitin ligase complex. Proc. Natl. Acad. Sci. USA **96:**12436–12441.
26. **Iyer, N. V., L. E. Kotch, F. Agani, S. W. Leung, E. Laughner, R. H. Wenger, M. Gassmann, J. D. Gearhart, A. M. Lawler, A. Y. Yu, and G. L. Semenza.** 1998. Cellular and developmental control of O_2 homeostasis by hypoxia-inducible factor 1α. Genes Dev. **12:**149–162.
27. **Jaakkola, P., D. R. Mole, Y. M. Tian, M. I. Wilson, J. Gielbert, S. J. Gaskell, A. Kriegsheim, H. F. Hebestreit, M. Mukherji, C. J. Schofield, P. H. Maxwell, C. W. Pugh, and P. J. Ratcliffe.** 2001. Targeting of HIF-α to the von Hippel-Lindau ubiquitylation complex by O_2-regulated prolyl hydroxylation. Science **292:**468–472.
28. **Jiang, D., L. Zheng, and M. J. Lenardo.** 1999. Caspases in T-cell receptor-induced thymocyte apoptosis. Cell Death Differ. **6:**402–411.
29. **Kaelin, W. G., Jr.** 2002. Molecular basis of the VHL hereditary cancer syndrome. Nat. Rev. Cancer **2:**673–682.
30. **Kojima, H., H. Gu, S. Nomura, C. C. Caldwell, T. Kobata, P. Carmeliet, G. L. Semenza, and M. V. Sitkovsky.** 2002. Abnormal B lymphocyte development and autoimmunity in hypoxia-inducible factor 1α-deficient chimeric mice. Proc. Natl. Acad. Sci. USA **99:**2170–2174.
31. **Laird, P. W., A. Zijderveld, K. Linders, M. A. Rudnicki, R. Jaenisch, and A. Berns.** 1991. Simplified mammalian DNA isolation procedure. Nucleic Acids Res. **19:**4293.
32. **Latif, F., K. Tory, J. Gnarra, M. Yao, F. M. Duh, M. L. Orcutt, T. Stackhouse, I. Kuzmin, W. Modi, L. Geil, et al.** 1993. Identification of the von Hippel-Lindau disease tumor suppressor gene. Science **260:**1317–1320.
33. **Lee, P. P., D. R. Fitzpatrick, C. Beard, H. K. Jessup, S. Lehar, K. W. Makar, M. Perez-Melgosa, M. T. Sweetser, M. S. Schlissel, S. Nguyen, S. R. Cherry, J. H. Tsai, S. M. Tucker, W. M. Weaver, A. Kelso, R. Jaenisch, and C. B. Wilson.** 2001. A critical role for Dnmt1 and DNA methylation in T cell development, function, and survival. Immunity **15:**763–774.
34. **Ma, A., J. C. Pena, B. Chang, E. Margosian, L. Davidson, F. W. Alt, and C. B. Thompson.** 1995. Bclx regulates the survival of double-positive thymocytes. Proc. Natl. Acad. Sci. USA **92:**4763–4767.

35. **Makino, Y., H. Nakamura, E. Ikeda, K. Ohnuma, K. Yamauchi, Y. Yabe, L. Poellinger, Y. Okada, C. Morimoto, and H. Tanaka.** 2003. Hypoxia-inducible factor regulates survival of antigen receptor-driven T cells. J. Immunol. **171:**6534–6540.
36. **Malhotra, R., Z. Lin, C. Vincenz, and F. C. Brosius III.** 2001. Hypoxia induces apoptosis via two independent pathways in Jurkat cells: differential regulation by glucose. Am. J. Physiol. Cell Physiol. **281:**C1596–C1603.
37. **Maltepe, E., J. V. Schmidt, D. Baunoch, C. A. Bradfield, and M. C. Simon.** 1997. Abnormal angiogenesis and responses to glucose and oxygen deprivation in mice lacking the protein ARNT. Nature **386:**403–407.
38. **Maxwell, P. H., M. S. Wiesener, G. W. Chang, S. C. Clifford, E. C. Vaux, M. E. Cockman, C. C. Wykoff, C. W. Pugh, E. R. Maher, and P. J. Ratcliffe.** 1999. The tumour suppressor protein VHL targets hypoxia-inducible factors for oxygen-dependent proteolysis. Nature **399:**271–275.
39. **Micheau, O., E. Solary, A. Hammann, and M. T. Dimanche-Boitrel.** 1999. Fas ligand-independent, FADD-mediated activation of the Fas death pathway by anticancer drugs. J. Biol. Chem. **274:**7987–7992.
40. **Ohh, M., C. W. Park, M. Ivan, M. A. Hoffman, T. Y. Kim, L. E. Huang, N. Pavletich, V. Chau, and W. G. Kaelin.** 2000. Ubiquitination of hypoxia-inducible factor requires direct binding to the beta-domain of the von Hippel-Lindau protein. Nat. Cell Biol. **2:**423–427.
41. **Ohh, M., R. L. Yauch, K. M. Lonergan, J. M. Whaley, A. O. Stemmer-Rachamimov, D. N. Louis, B. J. Gavin, N. Kley, W. G. Kaelin, Jr., and O. Iliopoulos.** 1998. The von Hippel-Lindau tumor suppressor protein is required for proper assembly of an extracellular fibronectin matrix. Mol. Cell **1:**959–968.
42. **Opferman, J. T., and S. J. Korsmeyer.** 2003. Apoptosis in the development and maintenance of the immune system. Nat. Immunol. **4:**410–415.
43. **Pfander, D., T. Kobayashi, M. C. Knight, E. Zelzer, D. A. Chan, B. R. Olsen, A. J. Giaccia, R. S. Johnson, V. H. Haase, and E. Schipani.** 2004. Deletion of *Vhlh* in chondrocytes reduces cell proliferation and increases matrix deposition during growth plate development. Development **131:**2497–2508.
44. **Pugh, C. W., and P. J. Ratcliffe.** 2003. Regulation of angiogenesis by hypoxia: role of the HIF system. Nat. Med. **9:**677–684.
45. **Rathmell, J. C., and C. B. Thompson.** 1999. The central effectors of cell death in the immune system. Annu. Rev. Immunol. **17:**781–828.
46. **Richards, F. M., P. A. Crossey, M. E. Phipps, K. Foster, F. Latif, G. Evans, J. Sampson, M. I. Lerman, B. Zbar, N. A. Affara, et al.** 1994. Detailed mapping of germline deletions of the von Hippel-Lindau disease tumour suppressor gene. Hum. Mol. Genet. **3:**595–598.
47. **Ryan, H. E., J. Lo, and R. S. Johnson.** 1998. HIF-1 alpha is required for solid tumor formation and embryonic vascularization. EMBO J. **17:**3005–3015.
48. **Ryan, H. E., M. Poloni, W. McNulty, D. Elson, M. Gassmann, J. M. Arbeit, and R. S. Johnson.** 2000. Hypoxia-inducible factor-1α is a positive factor in solid tumor growth. Cancer Res. **60:**4010–4015.
49. **Rytomaa, M., L. M. Martins, and J. Downward.** 1999. Involvement of FADD and caspase-8 signalling in detachment-induced apoptosis. Curr. Biol. **9:**1043–1046.
50. **Salceda, S., and J. Caro.** 1997. Hypoxia-inducible factor 1α (HIF-1α) protein is rapidly degraded by the ubiquitin-proteasome system under normoxic conditions: its stabilization by hypoxia depends on redox-induced changes. J. Biol. Chem. **272:**22642–22647.
51. **Sambrook, J., and D. W. Russell.** 2001. Molecular cloning: a laboratory manual, 3rd ed. Cold Spring Harbor Laboratory Press, Cold Spring Harbor, N.Y.
52. **Sanchez, I., C. J. Xu, P. Juo, A. Kakizaka, J. Blenis, and J. Yuan.** 1999. Caspase-8 is required for cell death induced by expanded polyglutamine repeats. Neuron **22:**623–633.
53. **Scortegagna, M., K. Ding, Y. Oktay, A. Gaur, F. Thurmond, L. J. Yan, B. T. Marck, A. M. Matsumoto, J. M. Shelton, J. A. Richardson, M. J. Bennett, and J. A. Garcia.** 2003. Multiple organ pathology, metabolic abnormalities and impaired homeostasis of reactive oxygen species in *Epas1*$^{-/-}$ mice. Nat. Genet. **35:**331–340.
54. **Sebzda, E., S. Mariathasan, T. Ohteki, R. Jones, M. F. Bachmann, and P. S. Ohashi.** 1999. Selection of the T cell repertoire. Annu. Rev. Immunol. **17:**829–874.
55. **Semenza, G. L.** 2001. HIF-1 and mechanisms of hypoxia sensing. Curr. Opin. Cell Biol. **13:**167–171.
56. **Sheikh, M. S., M. J. Antinore, Y. Huang, and A. J. Fornace, Jr.** 1998. Ultraviolet-irradiation-induced apoptosis is mediated via ligand independent activation of tumor necrosis factor receptor 1. Oncogene **17:**2555–2563.
57. **Smiley, S. T., M. Reers, C. Mottola-Hartshorn, M. Lin, A. Chen, T. W. Smith, G. D. Steele, Jr., and L. B. Chen.** 1991. Intracellular heterogeneity in mitochondrial membrane potentials revealed by a J-aggregate-forming lipophilic cation JC-1. Proc. Natl. Acad. Sci. USA **88:**3671–3675.
58. **Strasser, A., A. W. Harris, and S. Cory.** 1991. bcl-2 transgene inhibits T cell death and perturbs thymic self-censorship. Cell **67:**889–899.
59. **Surh, C. D., and J. Sprent.** 1994. T-cell apoptosis detected in situ during positive and negative selection in the thymus. Nature **372:**100–103.
60. **Thornberry, N. A., T. A. Rano, E. P. Peterson, D. M. Rasper, T. Timkey, M. Garcia-Calvo, V. M. Houtzager, P. A. Nordstrom, S. Roy, J. P. Vaillancourt, K. T. Chapman, and D. W. Nicholson.** 1997. A combinatorial approach defines specificities of members of the caspase family and granzyme B. Functional relationships established for key mediators of apoptosis. J. Biol. Chem. **272:**17907–17911.
61. **Tibbetts, M. D., L. Zheng, and M. J. Lenardo.** 2003. The death effector domain protein family: regulators of cellular homeostasis. Nat. Immunol. **4:**404–409.
62. **Vande Velde, C., J. Cizeau, D. Dubik, J. Alimonti, T. Brown, S. Israels, R. Hakem, and A. H. Greenberg.** 2000. BNIP3 and genetic control of necrosis-like cell death through the mitochondrial permeability transition pore. Mol. Cell. Biol. **20:**5454–5468.
63. **Van Hooijdonk, C. A., C. P. Glade, and P. E. Van Erp.** 1994. TO-PRO-3 iodide: a novel HeNe laser-excitable DNA stain as an alternative for propidium iodide in multiparameter flow cytometry. Cytometry **17:**185–189.
64. **Vermes, I., C. Haanen, H. Steffens-Nakken, and C. Reutelingsperger.** 1995. A novel assay for apoptosis. Flow cytometric detection of phosphatidylserine expression on early apoptotic cells using fluorescein labelled Annexin V. J. Immunol. Methods **184:**39–51.
65. **Wenger, R. H.** 2002. Cellular adaptation to hypoxia: O_2-sensing protein hydroxylases, hypoxia-inducible transcription factors, and O_2-regulated gene expression. FASEB J. **16:**1151–1162.
66. **Wiesener, M. S., J. S. Jurgensen, C. Rosenberger, C. K. Scholze, J. H. Horstrup, C. Warnecke, S. Mandriota, I. Bechmann, U. A. Frei, C. W. Pugh, P. J. Ratcliffe, S. Bachmann, P. H. Maxwell, and K. U. Eckardt.** 2003. Widespread hypoxia-inducible expression of HIF-2α in distinct cell populations of different organs. FASEB J. **17:**271–273.